Available online at www.sciencedirect.com
ScienceDirect
C. R. Mecanique 335 (2007) 187–193
COMPTES RENDUS MECANIQUE
http://france.elsevier.com/direct/CRAS2B/

Intermittency and universality in a Lagrangian model of velocity gradients in three-dimensional turbulence

Laurent Chevillard, Charles Meneveau *

Department of Mechanical Engineering, the Johns Hopkins University, 3400 N. Charles Street, Baltimore, MD 21218, USA

Received 20 January 2007; accepted after revision 13 March 2007

Available online 24 April 2007

Presented by Geneviève Comte-Bellot

Abstract

The universality of intermittency in hydrodynamic turbulence is considered based on a recent model for the velocity gradient tensor evolution. Three possible versions of the model are investigated differing in the assumed correlation time-scale and forcing strength. Numerical tests show that the same (universal) anomalous relative scaling exponents are obtained for the three model variants. It is also found that transverse velocity gradients are more intermittent than longitudinal ones, whereas dissipation and enstrophy scale with the same exponents. The results are consistent with the universality of intermittency and relative scaling exponents, and suggest that these are dictated by the self-stretching terms that are the same in each variant of the model. ***To cite this article: L. Chevillard, C. Meneveau, C. R. Mecanique 335 (2007).***
© 2007 Académie des sciences. Published by Elsevier Masson SAS. All rights reserved.

Résumé

Intermittence et universalité d'un modèle lagrangien des gradients de vitesse en turbulence 3D. Le caractère universel du phénomène d'intermittence en turbulence est étudié à partir d'un modèle récent régissant l'évolution du tenseur des gradients de vitesse. Trois versions possibles du modèle, pour lesquelles les hypothèses retenues pour le temps de corrélation et l'amplitude du forçage sont différentes, sont analysées. Une intégration numérique des équations montre que les exposants anormaux des moments relatifs sont les mêmes pour les trois variantes du modèle. Il est de plus montré que les gradients transversaux de vitesse sont plus intermittents que les longitudinaux alors que la dissipation et l'enstrophie se comportent comme des lois de puissance de même exposant. Ces résultats sont cohérents avec l'universalité des exposants relatifs et suggèrent l'importance du terme d'auto-étirement, qui est identique dans les trois variantes du modèle. ***Pour citer cet article : L. Chevillard, C. Meneveau, C. R. Mecanique 335 (2007).***
© 2007 Académie des sciences. Published by Elsevier Masson SAS. All rights reserved.

Keywords: Turbulence; Intermittency; Geometry

Mots-clés : Turbulence ; Intermittence ; Géométrie

* Corresponding author.
E-mail addresses: chevillard@jhu.edu (L. Chevillard), meneveau@jhu.edu (C. Meneveau).

1631-0721/$ – see front matter © 2007 Académie des sciences. Published by Elsevier Masson SAS. All rights reserved.
doi:10.1016/j.crme.2007.03.002

1. Introduction

Progress in understanding the small-scale structure of three-dimensional turbulent flow requires the study of the velocity gradient tensor $A_{ij} = \partial u_i/\partial x_j$, where $\mathbf{u}$ denotes the velocity vector. In incompressible flow, $\mathbf{A}$ is trace-free, i.e. $A_{ii} = 0$. The dynamical evolution of $\mathbf{A}$ is obtained by taking the gradient of the Navier–Stokes equation:

$$\frac{\mathrm{d}A_{ij}}{\mathrm{d}t} = -A_{ik}A_{kj} - \frac{\partial^2 p}{\partial x_i \partial x_j} + \nu \frac{\partial^2 A_{ij}}{\partial x_k \partial x_k} \tag{1}$$

where $\mathrm{d}/\mathrm{d}t$ stands for the Lagrangian material derivative, p is the pressure divided by the density of the fluid and ν is the kinematic viscosity. Neglecting viscous effects and the anisotropic part of the pressure Hessian entering in Eq. (1) leads to a closed formulation of the dynamics of the velocity gradient tensor known as the Restricted-Euler (RE) equations [1,2]. RE equations predict several phenomena observed in various experimental [3,4] and numerical [5] studies of turbulence, such as preferential alignments of vorticity and preferential axisymmetric extension. Recently, a system of differential equations describing longitudinal and transverse velocity increments has been derived from this approximation and predicts non-Gaussian statistics (and in particular skewness) of the components of $\mathbf{A}$ [6]. However, in this system as well as in the RE equations, the neglect of anisotropic pressure Hessian and viscous effects leads to singularities and precludes the establishment of stationary statistics due to undamped effects of the self-stretching term. To address this deficiency of RE dynamics, and based on prior works [7–9], a new model has been proposed [10]: the Recent Fluid Deformation (RFD) closure. It models both pressure Hessian and viscous term entering in Eq. (1). The RFD closure is based on the dynamics and the geometry of the deformation experienced by the fluid during its most recent evolution. A de-correlation time scale τ entering the various closure terms has to be specified, as well as a Gaussian forcing term. It was shown [10] that the system with τ chosen equal to the Kolmogorov scale and a fixed Gaussian forcing amplitude, reproduces stationary statistics with a number of geometric features of the velocity gradient, as well as relative scaling exponents of high-order moments, in strikingly close agreement to experimental and numerical measurements for real Navier–Stokes turbulence at moderate Reynolds numbers.

In order to explore the possible universality properties of the model, in this Note we study two different choices for the time-scale and also explore the consequences of varying the amplitude of the forcing term. We pose the question of whether the anomalous scaling exponents vary from case to case, and also extend the analysis to include scaling properties of the dissipation.

The model proposed by Ref. [10] begins with a change of variables, expressing the pressure in terms of the Lagrangian coordinates $\mathbf{X}$. One may define a mapping $\mathcal{M}_{t_0,t}$ between Eulerian and Lagrangian coordinates: $\mathcal{M}_{t_0,t} : \mathbf{X} \in \mathbb{R}^3 \mapsto \mathbf{x} \in \mathbb{R}^3$, where $\mathbf{x}(\mathbf{X}, t)$ denotes the position at a time t of a fluid particle which was at the position $\mathbf{x}(\mathbf{X}, t_0) = \mathbf{X}$ at the initial time t_0. The Jacobian matrix of the inverse mapping obeys $\mathrm{d}/\mathrm{d}t\,(\partial X_p/\partial x_i) = -A_{ki}(\partial X_p/\partial x_k)$. As argued before [10], for a relative short period of time (typically when $t - t_0 = \tau$, where τ is a characteristic Lagrangian decorrelation time scale for the velocity gradient tensor), the solution can be approximated as the matrix exponential of the velocity gradient itself, namely $(\partial X_p/\partial x_i) = (\exp[-\tau \mathbf{A}])_{pi}$.

With an Eulerian–Lagrangian change of variables, the pressure Hessian can be written in the following way:

$$\frac{\partial^2 p(t)}{\partial x_i \partial x_j} \approx \frac{\partial X_p}{\partial x_i}\frac{\partial X_q}{\partial x_j}\frac{\partial^2 p(t)}{\partial X_p \partial X_q} \approx -\frac{\mathrm{Tr}(\mathbf{A}^2)}{\mathrm{Tr}(\mathbf{C}_\tau^{-1})}\left(\mathbf{C}_\tau^{-1}\right)_{ij} \tag{2}$$

In the first approximation, spatial gradients of $(\partial X_p/\partial x_i)$ have been neglected [10]. In the second approximation, the short-time solution for $(\partial X_p/\partial x_i)$ mentioned before, the isotropy assumption for the Lagrangian pressure Hessian ($\partial^2 p/\partial X_p \partial X_q \sim \delta_{pq}$), and the trace-free condition of A_{ij} have been used. Moreover, $\mathbf{C}_\tau$ is the short-time Cauchy–Green tensor [10]: $\mathbf{C}_\tau = \mathrm{e}^{\tau \mathbf{A}}\mathrm{e}^{\tau \mathbf{A}^T}$. This model (Eq. (2)) can be viewed as a local version of the 'tetrad model' [8]. The time-scale τ is a model parameter and can be viewed as a characteristic time scale of the small dissipative scales of turbulence. Recent material deformation history can also be used to model other Hessian tensors entering in the Navier–Stokes equation (Eq. (1)) such as the viscous part. The resulting Hessian of $\mathbf{A}$ is modeled as a friction term and the characteristic time scale entering in the description is given by the (Reynolds number independent) integral time scale T [10]:

$$\nu \nabla^2 \mathbf{A} \approx -\frac{1}{T}\frac{\mathrm{Tr}(\mathbf{C}_\tau^{-1})}{3}\mathbf{A} \tag{3}$$

which is a stationary version of the model of Jeong and Girimaji [9]. Finally, combining Eqs. (2) and (3) into Eq. (1), one obtains a model for the dynamic evolution of $\mathbf{A}$ along a Lagrangian trajectory [10],

$$\mathrm{d}\mathbf{A} = \left(-\mathbf{A}^2 + \frac{\mathrm{Tr}(\mathbf{A}^2)}{\mathrm{Tr}(\mathbf{C}_\tau^{-1})}\mathbf{C}_\tau^{-1} - \frac{1}{T}\frac{\mathrm{Tr}(\mathbf{C}_\tau^{-1})}{3}\mathbf{A}\right)\mathrm{d}t + \mathrm{d}\mathbf{W} \tag{4}$$

A stochastic forcing term $\mathrm{d}\mathbf{W}$ has been added to model the combined action of large-scale forcing and neighboring eddies. The time evolution of $\mathbf{A}$ (Eq. (4)) is thus given by eight independent coupled ordinary (or stochastic depending on the forcing $\mathrm{d}\mathbf{W}$) differential equations.

In order to understand the roles played by the pressure Hessian (Eq. (2)) and the viscous term (Eq. (3)) in Eq. (4), some analysis can be carried out. Doing so for arbitrary initial conditions $\mathbf{A}(0)$ is difficult analytically because of the high dimension of the phase space. However, following Ref. [8] one may consider the decaying case (with $\mathrm{d}\mathbf{W} = 0$) along a particular direction corresponding to strain with two equal positive, and one negative, eigenvalues. Along this direction on the 'Vieillefosse tail', the tensor $\mathbf{A}$ and the evolution of the relevant eigenvalue $\lambda(t)$ from the model (Eq. (4)) are given by

$$\mathbf{A} = \begin{pmatrix} \lambda(t) & 0 & 0 \\ 0 & \lambda(t) & 0 \\ 0 & 0 & -2\lambda(t) \end{pmatrix} \quad \overset{\mathrm{d}\mathbf{W}=0}{\Rightarrow} \quad \frac{\mathrm{d}\lambda}{\mathrm{d}t} = \frac{4\mathrm{e}^{-2\tau\lambda} - \mathrm{e}^{4\tau\lambda}}{2\mathrm{e}^{-2\tau\lambda} + \mathrm{e}^{4\tau\lambda}}\lambda^2 - \frac{2\mathrm{e}^{-2\tau\lambda} + \mathrm{e}^{4\tau\lambda}}{3T}\lambda \tag{5}$$

The solution of the ODE in Eq. (5) is such that $\lambda(t)$ retains the same sign as $\lambda(0)$. Let us also recall that in the RE system, i.e. $\mathrm{d}\mathbf{A}/\mathrm{d}t = -\mathbf{A}^2 + \mathbf{I}\,\mathrm{Tr}(\mathbf{A}^2)/3$, the time evolution of λ is simply given by $\mathrm{d}\lambda/\mathrm{d}t = \lambda^2$ and the finite time divergence is given by the solution $\lambda(t) = \lambda(0)/(1 - t\lambda(0))$ in a finite time $1/\lambda(0)$. In our case, we see from Eq. (5) that the anisotropic part of the pressure Hessian acts directly against the development of the singularity induced by the self-stretching term. Indeed, the coefficient in front of λ^2 is bounded between $[-1; 1]$. Thus this model for pressure Hessian can regularize the finite time divergence when $\lambda \gg \tau^{-1}$ since then the prefactor of λ^2 is close to -1 and the solution of $\mathrm{d}\lambda/\mathrm{d}t = -\lambda^2$ tends to zero at large times. Further discussions of the regularization along the Vieillefosse tail require specification of the time scale τ, in particular its dependence on the Reynolds number.

2. Reynolds number effects, intermittency, and relative anomalous scaling

In this section, three choices to model Reynolds number changes are considered: (I) constant Kolmogorov time scale (this was the case studied in [10] and for clarity the relevant results will be repeated here), (II) local time scale, and (III) variable forcing strength.

Intermittency is studied by examining the scaling of moments of velocity gradients. As in [10] we consider both longitudinal (A_{ii}, no index summation) and transverse (A_{ij}, $i \neq j$) gradients. Nelkin [11] shows, assuming the relevance of the multifractal formalism in the inertial range, that the relative scaling of higher order moments of velocity derivatives should behave as a power law

$$\left\langle |A_{ij}|^p \right\rangle \sim \left\langle |A_{ij}|^2 \right\rangle^{\mathcal{F}^{L,T}(p)/2}, \quad \text{with } \mathcal{F}^{L,T}(p) = \min_h \left[-\frac{p(h-1) + 1 - \mathcal{D}^{L,T}(h)}{h+1} \right] \tag{6}$$

These equations are written for either longitudinal ($i = j$, superscript L) or transverse ($i \neq j$, superscript T) gradients. The functions $\mathcal{D}^L(h)$ and $\mathcal{D}^T(h)$ are the longitudinal and transverse singularity spectrum, respectively. Imposing a 3rd-order velocity structure function exponent of 1 in the inertial range (which is exact for longitudinal velocity increments, and a good approximation for transverse ones) leads to $\langle (A_{ij})^2 \rangle \sim \mathcal{R}_e$, i.e. finiteness of dissipation is recovered [12].

To proceed and facilitate interpretation of results, as in Ref. [10] we choose a simple quadratic form for the singularity spectrum $\mathcal{D}^{L,T}(h) = 1 - (h - c_1^{L,T})^2/(2c_2^{L,T})$, with $c_1^{L,T} = \frac{1}{3} + \frac{3}{2}c_2^{L,T}$ where the parameter $c_2^{L,T}$ is called the intermittency exponent (see Ref. [13] for further details).

Case I. Constant Kolmogorov time scale: First we consider the simplest case in which τ is a constant value. Because τ should scale with the Lagrangian decorrelation time-scale of the velocity gradients, it is chosen to be of the order of the Kolmogorov time scale τ_K [10]. This choice gives an explicit Reynolds number dependence to the model since it that case, $\tau_K \sim \mathcal{R}_e^{-1/2}$. As argued earlier already, from Eq. (5), we see that when $\lambda \gg \tau^{-1}$, the model pressure Hessian causes the coefficient appearing in front of λ^2 to switch from 1 to -1. Thus, it acts to counteract the finite

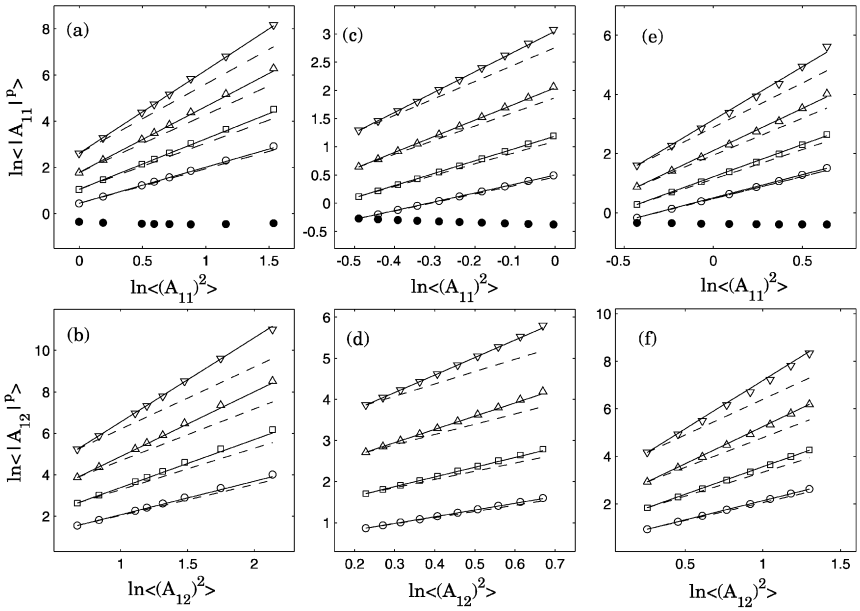

Fig. 1. Relative scaling properties of higher order moments, i.e. $\ln\langle|A_{ij}|^p\rangle$, as a function of the second order moment $\ln\langle|A_{ij}|^2\rangle$. Dashed-line represents K41 predictions (i.e. $p/2$). Solid lines: multifractal predictions (i.e. $\mathcal{F}(p)/2$, see text), and $\circ$ ($p=3$), $\square$ ($p=4$), $\triangle$ ($p=5$) and $\triangledown$ ($p=6$). Skewness of longitudinal components is represented with $\bullet$. Case I (a), (b): $\Gamma \equiv \tau_K/T = 0.2$, 0.15, 0.1, 0.09, 0.08, 0.07, 0.06 and 0.05 (same value as in Ref. [10]). Case II (c), (d): Local time scale $\Gamma/\sqrt{2\,\mathrm{Tr}(\mathbf{S}^2)}$ with $\Gamma = 1.4$; 1.35; 1.3; 1.25; 1.2; 1.15; 1.1; 1.05; 1 and 0.95. Case III (e), (f): Local time scale $1/\sqrt{2\,\mathrm{Tr}(\mathbf{S}^2)}$ with increasing variance of the forcing term $\mathrm{d}\mathbf{W} = \sigma\mathbf{G}\sqrt{2\,\mathrm{d}t}$, with $4\sigma^2 = 3$; 3.5; 4; 4.5; 5; 5.5; 6; 6.5. All parameters listed correspond to points going from left to right.

Fig. 1. Comportement des moments d'ordres supérieurs, c'est-à-dire $\ln\langle|A_{ij}|^p\rangle$, relativement au moment d'ordre 2, $\ln\langle|A_{ij}|^2\rangle$. Les prédictions de K41 (c'est-à-dire $p/2$) sont représentées à l'aide d'une ligne discontinue. Les prédictions du formalisme multifractal (i$\mathcal{F}(p)/2$, voir le corps du texte), sont indiquées par une ligne continue. Les symboles utilisés pour représenter l'estimation des moments d'ordre p sont $\circ$ ($p=3$), $\square$ ($p=4$), $\triangle$ ($p=5$) et $\triangledown$ ($p=6$). L'asymétrie des composantes longitudinales est indiquée par $\bullet$. Cas I (a), (b) : $\Gamma \equiv \tau_K/T = 0.2$, 0.15, 0.1, 0.09, 0.08, 0.07, 0.06 and 0.05 (les mêmes valeurs que dans la Ref. [10]). Cas II (c), (d) : Echelle temporelle locale $\Gamma/\sqrt{2\,\mathrm{Tr}(\mathbf{S}^2)}$ avec $\Gamma = 1.4$; 1.35; 1.3; 1.25; 1.2; 1.15; 1.1; 1.05; 1 and 0.95. Cas III (e), (f) : Echelle temporelle locale $1/\sqrt{2\,\mathrm{Tr}(\mathbf{S}^2)}$ et différentes variances du terme de forçage $\mathrm{d}\mathbf{W} = \sigma\mathbf{G}\sqrt{2\,\mathrm{d}t}$, avec $4\sigma^2 = 3$; 3.5; 4; 4.5; 5; 5.5; 6; 6.5. Tous les paramètres énumérés avec l'ordre indiqué correspondent aux symboles placés de la gauche vers la droite.

time divergence and causes λ to decrease in time as $1/t$. The viscous part is also very important and can be seen as a very efficient damping term with a coefficient which grows exponentially with increasing λ's. We have checked numerically that for any initial conditions, the system (5) is such that $\lambda(t) \to 0$ when $t \to +\infty$. The divergence is thus regularized. We have also checked numerically that for any other initial conditions for $\mathbf{A}$, i.e. those which cannot be written as in Eq. (5), all components of $\mathbf{A}$ evolving under Eq. (4) tend to zero in the absence of forcing. Without loss of generality, henceforth all variables will be scaled with the time-scale T, i.e. $t/T \to t$ and $A_{ij}T \to A_{ij}$. Let us denote by $\Gamma = \tau/T$ the only free parameter. The forcing term $\mathrm{d}\mathbf{W} = \mathbf{G}\sqrt{2\,\mathrm{d}t}$ is Gaussian and its covariance matrix is assumed to be Reynolds number independent (see Ref. [10] for details). The model (Eq. (4)) is solved numerically according to Ref. [10] and stationary statistics are obtained. The results are examined from the point of view of intermittency and anomalous relative scaling properties.

To facilitate comparison with the cases considered in II and III, in Fig. 1(a), (b) we present one of the results of Ref. [10]. These results are obtained from numerical integration of the model system over long periods of time and the evaluation of moments of various orders. Clearly, intermittency is predicted because the K41 line (i.e. of slope $p/2$, dashed lines) does not fit the computed results from the model. We display (solid lines) various predictions obtained with the help of Eq. (6). The results can be described well with the parameters $c_2^L = 0.025$ and $c_2^T = 0.040$ for the longitudinal and transverse cases, respectively. Transverse gradients appear to be more intermittent than longitudinal ones. Also, as shown in Ref. [10] longitudinal gradients PDF is skewed. As was stressed in Ref. [10], the intermittency parameters c_2^L and c_2^T are very close to those obtained from experimental data, see Refs. [13,14]. As remarked in Ref. [10], however, for values of τ/T smaller than about 0.05 (corresponding to a Taylor-based Reynolds number of

order 300 [15]) the predicted statistics become unrealistic. Still, the fact that a model with only 8 degrees of freedom derived directly from the Navier–Stokes equations predicts realistic relative intermittency exponents (albeit in a limited range of Reynolds numbers) is quite remarkable. The results raise the question of how robust these findings are with respect to other possible choices of the time-scale and forcing strengths. This is considered in the next two subsections.

Case II. Reynolds number dependent local time scale: It has been hypothesized that the dissipative scale in turbulence is not constant but fluctuates due to the intermittency phenomenon [16]. Consistent with this notion of a local fluctuating cutoff scale, here we choose $\tau(t) = \Gamma(\mathcal{R}_e)/\sqrt{2\,\mathrm{Tr}(\mathbf{S}^2)}$ where Γ is a dimensionless parameter, and an unknown function of the Reynolds number. Hence in this case, as opposed to Case I where τ was held constant, the time-scale fluctuates, being a function the variable velocity gradients. When Γ decreases for a fixed $\mathbf{A}$, the predicted pressure Hessian is closer to isotropy. Then the system (4) is dominated more by the quadratic (singularity-inducing) self-stretching term, which is what one may expect at higher Reynolds numbers. In this case, for a fluctuating dissipative time scale, the ODE appearing in equation (4) can be solved exactly and one obtains

$$\lambda(t) = \frac{\lambda(0)b^2}{3a\lambda(0) - \mathrm{e}^{\frac{b}{3}t}(-b^2 + 3a\lambda(0))}, \quad \text{where } a = 4\mathrm{e}^{-\frac{2}{\sqrt{12}}\Gamma} - \mathrm{e}^{\frac{4}{\sqrt{12}}\Gamma} \text{ and } b = 2\mathrm{e}^{-\frac{2}{\sqrt{12}}\Gamma} + \mathrm{e}^{\frac{4}{\sqrt{12}}\Gamma} > 0 \tag{7}$$

The long time behavior of the solution depends on the sign of the constant a. For $\Gamma > \frac{\sqrt{12}}{6}\ln 4 \approx 0.80$, $\lambda(t) \to 0$ at large times. For smaller Γ's, the solution diverges in a finite time (when $\lambda(0) > b^2/(3a)$) and the model is unable to regularize the divergence predicted by the self-stretching term. Therefore, similarly to the constant Kolmogorov time-scale option considered in I, this approach appears not to allow reaching arbitrarily high Reynolds numbers. The system using different values of Γ is integrated numerically as in I, with the same Gaussian forcing $\mathrm{d}\mathbf{W} = \mathbf{G}\sqrt{2\,\mathrm{d}t}$. Resulting moments of velocity gradients are displayed in Fig. 1(c), (d). As in I, anomalous relative scaling and intermittency is obtained. The solid lines again are obtained by using a longitudinal intermittency coefficients $c_2^L = 0.025$, the same as the one obtained with a constant time scale. The transverse coefficient is $c_2^T = 0.045$, also almost the same as that obtained in I.

Case III. Variable forcing strength: Another option to model Reynolds number effects is to vary the strength of the stochastic forcing through the term $\mathrm{d}\mathbf{W} = \sigma\mathbf{G}\sqrt{2\,\mathrm{d}t}$. The variance σ^2 is assumed to increase with increasing Reynolds number based on the notion that the relative strength of forcing (compared to viscous term) from neighbouring and large eddies increases with Reynolds number. The explicit dependence on Reynolds number is unknown but since we use relative scaling, the precise relationship with Reynolds number is not needed for the analysis. As a time-scale, in this case we use the local time scale, namely $\tau(t) = 1/\sqrt{2\,\mathrm{Tr}(\mathbf{S}^2)}$, i.e. the former time scale of Eq. (7) with $\Gamma = 1$ (which is large enough to insure regularization along the Vieillefosse tail). Numerically it is observed that increased σ leads to increased variance of the velocity gradient components. This is consistent with the view that changing the forcing may be viewed as modifying the effective Reynolds number.

Numerical results for the moments of gradients and quantification of relative scaling are presented in Fig. 1(e), (f) for various strengths σ of the forcing. Once again, using the representation of Eq. (6), the results agree very well with intermittent exponents consistent with $c_2^L = 0.025$ and $c_2^T = 0.040$. Thus the quantitative predictions of anomalous relative scaling in the model appear to be quite robust with regard to details of the regularization time-scale and forcing.

3. Relative scaling properties of dissipation and enstrophy

The model (Eq. (4)) can also be used to predict the dynamics and statistics of several norms of the velocity gradient tensor, namely $E_\epsilon = 2\,\mathrm{Tr}(\mathbf{S}^2)$ (the dissipation divided by viscosity), $E_\zeta = 2\,\mathrm{Tr}(\mathbf{\Omega}\mathbf{\Omega}^T)$ (the enstrophy, where $\mathbf{\Omega}$ is the antisymmetric part of $\mathbf{A}$) and $E_\varphi = \mathrm{Tr}(\mathbf{A}\mathbf{A}^T)$ (the 'pseudo-dissipation' divided by viscosity). It is well known that in turbulent flows, these 'dissipation fields' are highly intermittent [12,17,18]. In homogeneous and isotropic turbulence, $\langle E_\epsilon\rangle = \langle E_\zeta\rangle = \langle E_\varphi\rangle$, while higher order moments of these quantities are not similarly linked. We will perform then, in a similar fashion as Fig. 1, a relative scaling study of these quantities.

We present in Fig. 2, similar to Fig. 1, the numerical results for relative scaling of E_ϵ and E_ζ obtained from a numerical integration of the model (Eq. (4)), for the three cases I, II and III. Clearly, numerical results do not follow K41 predictions (dashed line). It is found that for all three cases the relative scaling properties are the same, i.e. again we observe robustness with respect to how Reynolds number effects are modeled. Finally, we observe

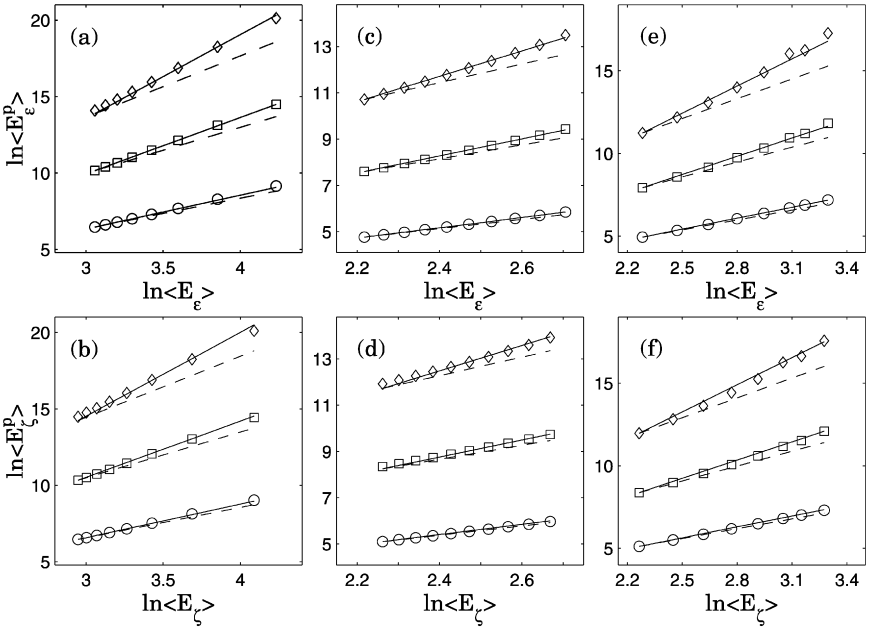

Fig. 2. Relative scaling properties of higher order moments, i.e. $\ln\langle E^p\rangle$, as a function of $\ln\langle E\rangle$, where E stands for 'dissipation' E_ϵ or 'enstrophy' E_ζ. The cases (a)–(f) correspond to the same model parameters as in Fig. 1. Various orders of moments $\langle E^p\rangle$ are studied: $p = 2$ (∘), $p = 3$ (□) and $p = 4$ (⋄). Dashed-line represents K41 predictions (i.e. slope p), solid lines multifractal predictions (i.e. slope $p + \mathcal{F}(p)$, see footnote 1).

Fig. 2. Comportement des moments d'ordres supérieurs, c'est-à-dire $\ln\langle E^p\rangle$, relativement à la moyenne, $\ln\langle E\rangle$, E signifiant la « dissipation » E_ϵ ou l'« enstrophie » E_ζ. Les figures (a)–(f) correspondent au même jeu de paramètres utilisé dans la Fig. 1. Les ordres des moments sont indiqués par $p = 2$ (∘), $p = 3$ (□) and $p = 4$ (⋄). La ligne discontinue représente la prédiction de K41 (de pente p), la ligne continue correspondant aux prédictions multifractales (de pente $p + \mathcal{F}(p)$, voir remarque 1).

that dissipation and enstrophy scale the same. The solid line shows the multifractal predictions[1] [19–21], using a unique intermittency parameter $\mu = 0.25$. Similar results are obtained when studying the relative scaling properties of the pseudo-dissipation E_φ, i.e. we obtain $\mu \approx \mu^\varphi \approx 0.25$ (data not shown). Thus, in the model the dissipation, enstrophy and 'pseudo-dissipation' display the same or very similar intermittency exponents. The value of $\mu \approx 0.25$ is in excellent agreement with previous numerical and experimental investigations [12,18].

4. Summary and conclusions

Several options to represent Reynolds number in a Lagrangian velocity gradient model using the newly proposed RFD closure [10] have been considered. Numerical integrations of the model show that three different ways to represent Reynolds number variations have led to the same (universal) intermittency relative scaling exponents. Consistent with data, it has been found that longitudinal intermittency exponent is of order $c_2^L = 0.025$ and the transverse one is $c_2^T = 0.040$. Relative scaling analysis for dissipation, enstrophy and pseudo-dissipation shows that all three quantities share the same intermittency coefficient ($\mu \approx 0.25$) in the model predictions. The universality of the results highlights the importance of the self-stretching term in the dynamics of $\mathbf{A}$. Future work will be devoted to test the robustness of the predicted intermittency phenomenon with respect to possible modifications of this term.

At this stage it may be of interest to recall some prior discussions dealing with the various scaling exponents in turbulence. On the one hand, and in agreement with our model results, numerically and experimentally the longitudinal

[1] Multifractal predictions for relative scaling properties of the dissipation signals E (either E_ϵ, E_ζ or E_φ) may be derived in analogy with Eq. (6) [19–21]: $\langle E^p\rangle \sim \langle E\rangle^{p+\mathcal{F}(p)}$, with $\mathcal{F}(p) = \min_\alpha[-3(p(\alpha-1)+3-f(\alpha))/(\alpha+3)]$. The singularity spectrum $f(\alpha)$ is such that $\mathcal{F}(p)$ vanishes for both $p = 0$ and $p = 1$. Assuming furthermore a simple parabolic form for $f(\alpha)$, we are left with a unique parameter μ usually called the intermittency parameter in the literature [12]: $f(\alpha) = 3 - [\alpha - (1+\mu)]^2/(2\mu)$. The set of exponents $\mathcal{F}(p)$, $f(\alpha)$, and μ may in principle differ for each of the fields E_ϵ, E_ζ and E_φ.

and transverse velocity gradient intermittencies were found to be different (see for instance Ref. [22] for a recent review on the subject). Conversely (and unlike our model's results), they have been predicted to be the same from a field theoretic approach (see Ref. [23] and references therein). On the other hand, unlike our model results, enstrophy was found to be more intermittent than dissipation in numerical flows [24] (and in experiments, albeit using only a single component of vorticity [17]), whereas (in agreement with our model) they are predicted to scale the same at infinite Reynolds numbers from simple arguments based on the finiteness of the inertial range pressure spectrum [25], or from more systematic irreducible group representations [23]. It is therefore interesting to note that the present model provides, for a limited range of Reynolds numbers, an example of dynamics of the velocity gradient tensor in which transverse velocity gradients are more intermittent than longitudinal ones, whereas dissipation and enstrophy scale the same. Clearly more research is needed to elucidate the relationships between various exponents characterizing intermittency in turbulence, and possibly to clarify generalizations of the refined similarity hypothesis (e.g. such as in [24]). The present approach of using Lagrangian dynamical evolution equations [10] should help shed new light on this long-standing, important problem.

Acknowledgements

We thank M. Nelkin for motivating us to examine scaling properties of dissipation and enstrophy, and Y. Li, Z. Xiao, L. Biferale, S. Chen, G. Eyink and F. Toschi for useful suggestions. L.C. is supported by postdoctoral Fellowship from the Keck Fundation and C.M. by the National Science Foundation.

References

[1] P. Vieillefosse, Internal motion of a small element of fluid in an inviscid flow, Physica A 125 (1984) 150.
[2] B.J. Cantwell, Exact solution of a restricted Euler equation for the velocity gradient, Phys. Fluids A 4 (1992) 782.
[3] F. van der Bos, B. Tao, C. Meneveau, J. Katz, Effects of small-scale turbulent motions on the filtered velocity gradient tensor as deduced from holographic particle image velocimetry measurements, Phys. Fluids 14 (2002) 2457.
[4] B.W. Zeff, D.D. Lanterman, R. McAllister, R. Roy, E.J. Kostelich, D.P. Lathrop, Measuring intense rotation and dissipation in turbulent flows, Nature 421 (2003) 146.
[5] B.J. Cantwell, On the behavior of velocity gradient tensor invariants in direct numerical simulations of turbulence, Phys. Fluids A 5 (1993) 2008.
[6] Y. Li, C. Meneveau, Intermittency trends and Lagrangian evolution of non-Gaussian statistics in turbulent flow and scalar transport, J. Fluid Mech. 558 (2006) 133.
[7] S.S. Girimaji, S.B. Pope, A diffusion model for velocity gradients in turbulence, Phys. Fluids A 2 (1990) 242.
[8] M. Chertkov, A. Pumir, B.I. Shraiman, Lagrangian tetrad dynamics and the phenomenology of turbulence, Phys. Fluids 11 (1999) 2394.
[9] E. Jeong, S.S. Girimaji, Velocity-gradient dynamics in turbulence: effect of viscosity and forcing, Theor. Comput. Fluid Dynam. 16 (2003) 421.
[10] L. Chevillard, C. Meneveau, Lagrangian dynamics and statistical geometric structure of turbulence, Phys. Rev. Lett. 97 (2006) 174501.
[11] M. Nelkin, Multifractal scaling of velocity derivatives in turbulence, Phys. Rev. A 42 (1990) 7226.
[12] U. Frisch, Turbulence, Cambridge Univ. Press, Cambridge, 1995.
[13] L. Chevillard, B. Castaing, E. Lévêque, A. Arneodo, Unified multifractal description of velocity increments statistics in turbulence: Intermittency and skewness, Physica D 218 (2006) 77.
[14] B. Dhruva, Y. Tsuji, K.R. Sreenivasan, Transverse structure functions in high-Reynolds-number turbulence, Phys. Rev. E 56 (1997) R4928.
[15] P.K. Yeung, S.B. Popem, B.L. Sawford, Reynolds number dependence of Lagrangian statistics in large numerical simulations of isotropic turbulence, J. Turbulence 7 (2006) 58.
[16] G. Paladin, A. Vulpiani, Degrees of freedom of turbulence, Phys. Rev. A 35 (1987) 1971.
[17] C. Meneveau, K.R. Sreenivasan, P. Kailasnath, M.S. Fan, Joint multifractal measures: Theory and applications to turbulence, Phys. Rev. A 41 (1990) 894.
[18] C. Meneveau, K.R. Sreenivasan, The multifractal nature of turbulent energy dissipation, J. Fluid Mech. 224 (1991) 429.
[19] K.R. Sreenivasan, C. Meneveau, Singularities of the equations of fluid motion, Phys. Rev. A 38 (1988) 6287.
[20] C. Meneveau, M. Nelkin, Attractor size in intermittent turbulence, Phys. Rev. A 39 (1989) 3732.
[21] M.S. Borgas, The multifractal Lagrangian nature of turbulence, Phil. Trans. R. Soc. Lond. A 342 (1993) 379.
[22] X.-Q. Jiang, H. Gong, J.-K. Liu, M.-D. Zhou, Z.-S. She, Hierarchical structures in a turbulent free shear flow, J. Fluid Mech. 569 (2006) 259.
[23] L. Biferale, I. Procaccia, Anisotropy in turbulent flows and in turbulent transport, Phys. Rep. 414 (2005) 43.
[24] S. Chen, K.R. Sreenivasan, M. Nelkin, N. Cao, Refined similarity hypothesis for transverse structure functions in fluid turbulence, Phys. Rev. Lett. 79 (1997) 2253.
[25] M. Nelkin, Enstrophy and dissipation must have the same scaling exponent in the high Reynolds number limit of fluid turbulence, Phys. Fluids 11 (1999) 2202.

Available online at www.sciencedirect.com
ScienceDirect
C. R. Mecanique 335 (2007) 737
COMPTES RENDUS MECANIQUE
http://france.elsevier.com/direct/CRAS2B/

Erratum

Corrigendum to the Note "Intermittency and universality in a Lagrangian model of velocity gradients in three-dimensional turbulence" [C. R. Mecanique 335 (4) (2007) 187–193]

Laurent Chevillard *, Charles Meneveau

Department of Mechanical Engineering, Johns Hopkins University, 3400 N. Charles Street, Baltimore, MD 21218, USA

Available online 21 September 2007

Presented by Geneviève Comte-Bellot

Since publication, we have found two typographical errors.

In Eq. (6) the exponent should be $\mathcal{F}^{L,T}(p)$ instead of $\mathcal{F}^{L,T}(p)/2$, and in the caption to Fig. 1 (second line), it should be $\mathcal{F}(p)$ instead of $\mathcal{F}(p)/2$.

DOI of original article: 10.1016/j.crme.2007.03.002.

* Corresponding author.
E-mail addresses: chevillard@jhu.edu (L. Chevillard), meneveau@jhu.edu (C. Meneveau).

1631-0721/$ – see front matter © 2007 Académie des sciences. Published by Elsevier Masson SAS. All rights reserved.
doi:10.1016/j.crme.2007.09.001